Supporting information

A tough organohydrogel-based multiresponsive sensor for a triboelectric nanogenerator and supercapacitor toward wearable intelligent devices

Kui Hu [a], Zhipeng Zhao [a], Yingyue Wang [a], Longhuo Yu [a], Kai Liu [a,*], Hui Wu [a], Liulian Huang [a], Lihui Chen [a], Yonghao Ni [a,b]

[a] College of Materials Engineering, Fujian Agriculture and Forestry University, Fuzhou, Fujian 350108, P. R. China

[b] Limerick Pulp and Paper Centre, Department of Chemical Engineering, University of New Brunswick, Fredericton, New Brunswick E3B5A3, Canada

Corresponding author:

Kai Liu

College of Materials Engineering, Fujian Agriculture and Forestry University, Fuzhou, Fujian 350108, P. R. China.

E-mail: liuk1103@163.com

This section includes:

organohydrogel-based TENG.

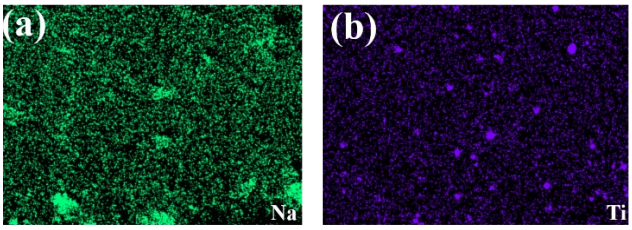

Figure S1. Mapping images of Na and Ti elements in the MGCSP organohydrogel.

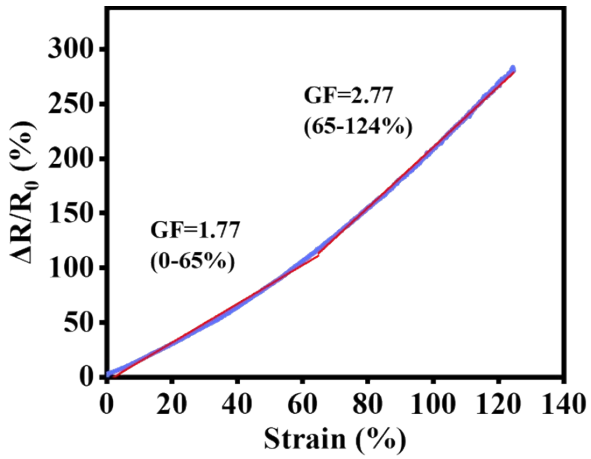

Figure S2. Relative resistance changes of the MGCSP organohydrogel to the applied strain.

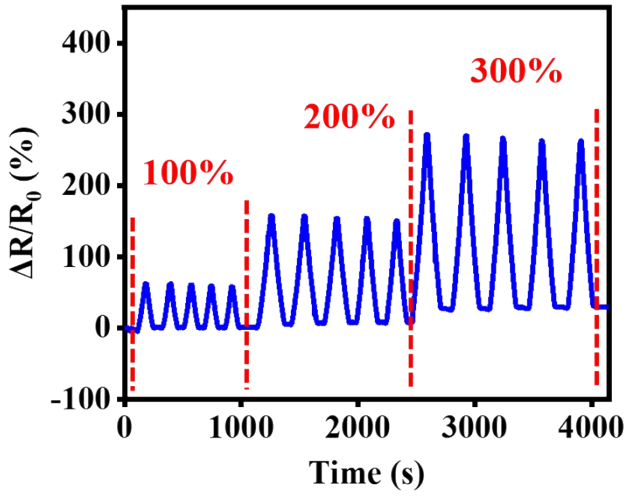

Figure S3. Relative resistance changes of the MGCSP organohydrogel-based sensor for loading of 100%, 200%, and 300% strain, respectively.

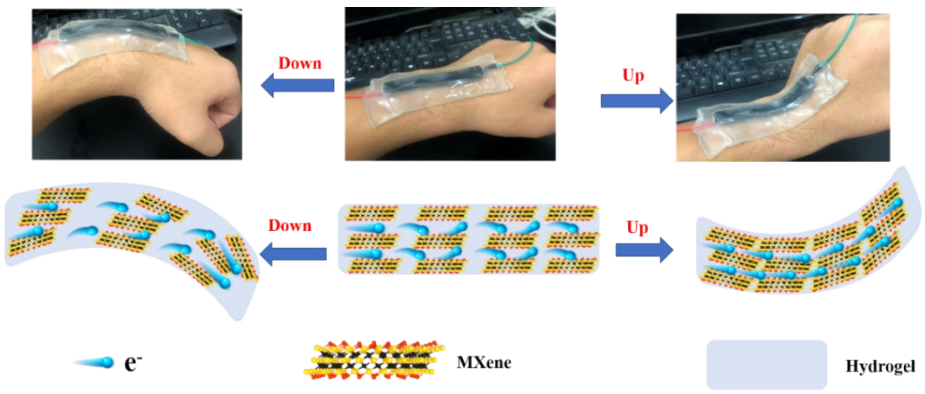

Figure S4. The formation of the conductive path constructed by MX-GO nanocomposites in the MGCSP organohydrogel.

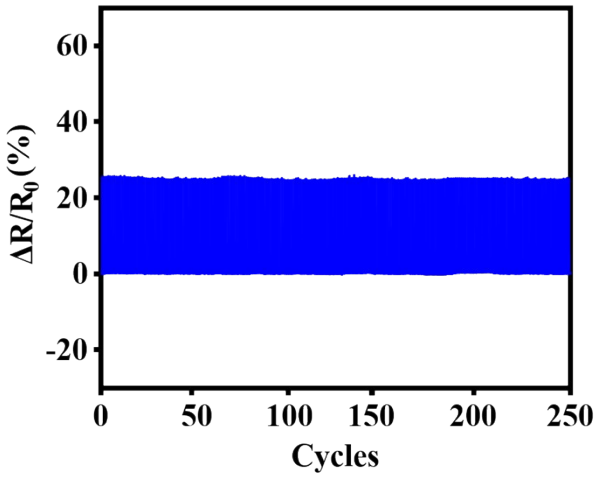

Figure S5. Relative resistance changes of the MGCSP organohydrogel at repeated 30% strain loading for 250 cycles.

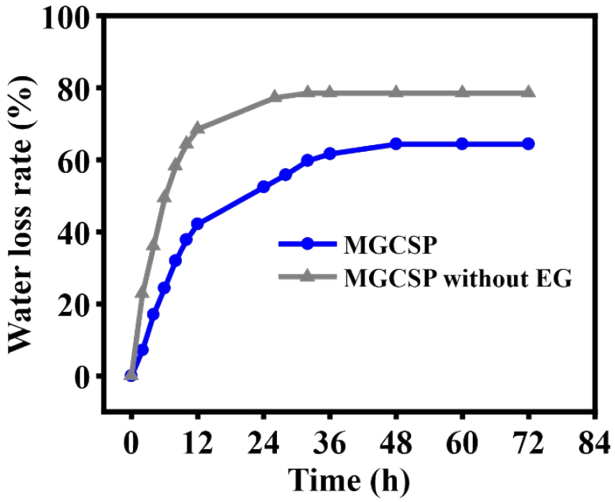

Figure S6. Water loss rate of the MGCSP organohydrogel with and without EG under constant temperature (25 ℃) and relative humidity (52%) conditions.

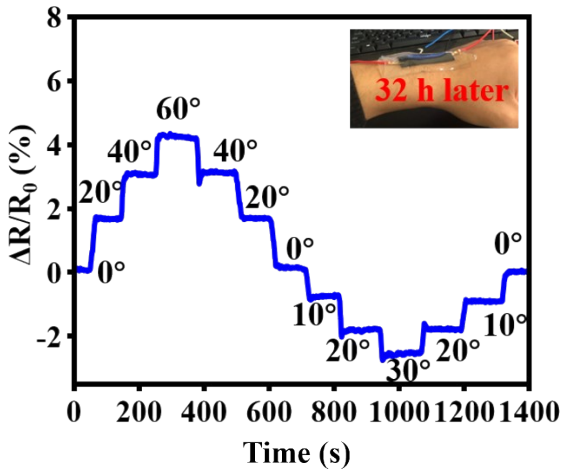

Figure S7. Relative resistance changes induced by the bending of the wrist at different flexion angles measured by the MGCSP organohydrogel-based sensor after storage at 25 ℃ for 32 h.

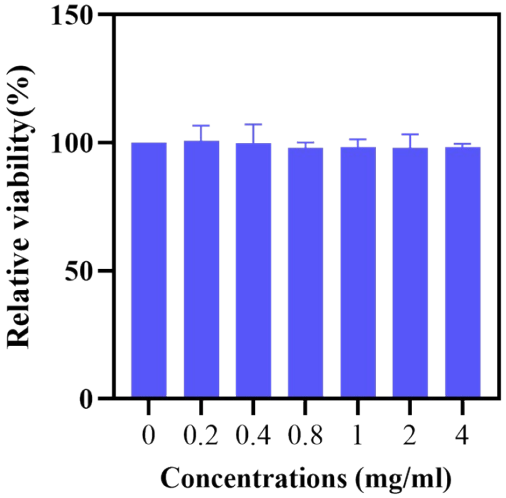

Figure S8. Evaluation of biocompatibility on NIH-3T3 cells cultured with different concentrations of extracts of the MGCSP organohydrogels.

The biocompatibility of the MGCSP organohydrogel on NIH 3T3 cells was evaluated by CCK-8 assay according to the literatures [1, 2], the relative viability was calculated by the following equation:

Relative viability $=(A_{sample})/(A_{control})\times 100\%$

where A_{sample} and $A_{control}$ were the absorbances in different concentrations of extracts of the MGCSP organohydrogel and cell culture medium, respectively.

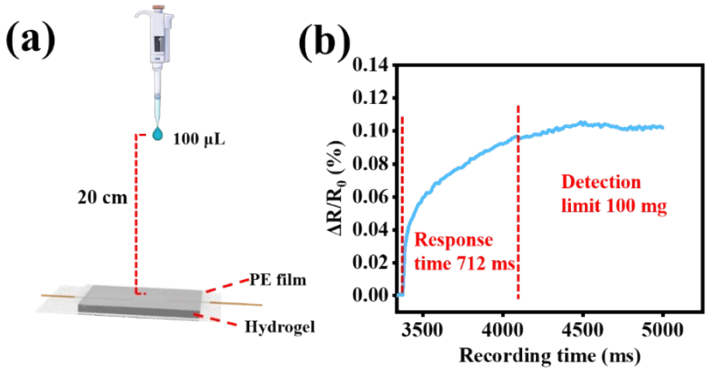

Figure S9. The measurement approach (a) and results (b) of the response time and detection limit of the MGCSP organohydrogel.

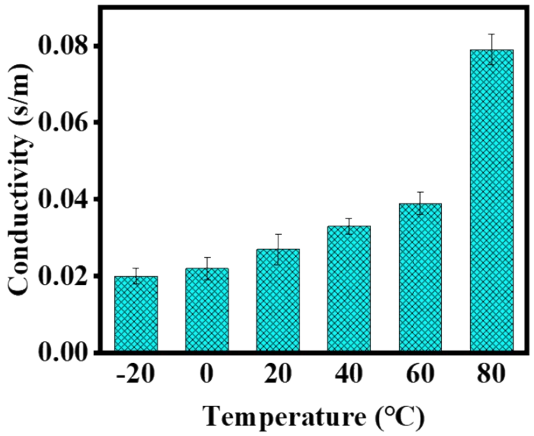

Figure S10. The conductivities of the MGCSP organohydrogel at different temperatures from -20 to 80 °C.

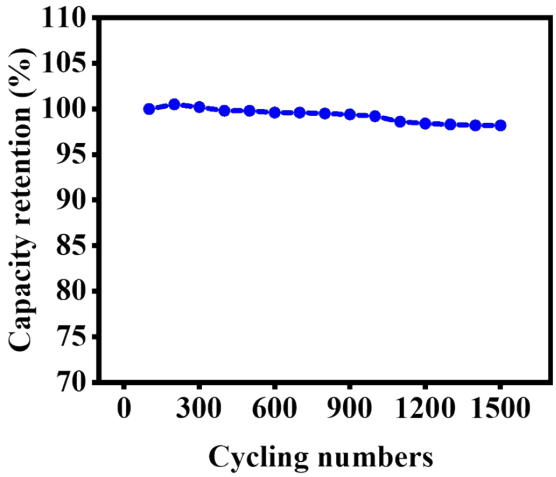

Figure S11. Capacitance retention of the supercapacitor after 1500 charging and discharging cycles at current density of 1 $A \cdot g^{-1}$.

Table S1. The compositions of P, SP, CSP, and MGCSP organohydrogel.

Hydrogels	PVA (g)	SA (g)	H_2O (g)	CNF (g)	MX-GO (g)	ethylene glycol (g)
P	12	0	40	0	0	4
SP	12	0.4	40	0	0	4
CSP	12	0.4	38	2	0	4
MGCSP	12	0.4	38	2	0.08	4

Table S2. The percentage of C-C, C-O, and -COO from the C 1s peaks of the dried MXene and MXene-GO nanocomposites XPS spectra.

Samples	**C-C (%)**	**C-O (%)**	**-COO (%)**
MXene	33.20	3.39	---
MXene-GO	46.59	20.23	3.65

Table S3. Comparation of GFs between the MGCSP organohydrogel and recently reported hydrogels.

Hydrogels	**Conductive component**	**Gauge factor**	**Reference**
PVA/Polyvinylpyrrolidone	Fe^{3+}	0.478 (200%)	[3]
PAAm	LiCl	0.84 (40%)	[4]
PAA	Al^{3+}	0.76 (75%)	[5]
PAA/PVA	Fe^{3+}/F-CNT	1.16 (101%)	[6]
PVA/HPC	NaCl	0.984 (100%)	[7]
PVA/SA	**GO-MXene**	**1.77 (0-65%)** **2.77 (65-124%)**	**This work**

Table S4. Comparation of V_{OC}, I_{SC} and Q_{SC} between the MGCSP organohydrogel-based TENG and the recently reported TENGs.

Conductive materials	**Friction materials**	**VOC** (V)	**ISC** (μA)	**QSC** (nC)	**Contact area**	**Reference**
PVA/PEI	PDMS/Skin	70	12.08	22	2.0×2.0 cm^{-2}	[8]
PVA/PDAP/MWCNT	Silicone rubber/Skin	95	1.5	32	30×30 mm^{-2}	[9]
PAAm-alginate hydrogel	PDMS/Skin	11.2	0.07	3.74	2.5×2.5 cm^{-2}	[10]
HTS-c-hydrogel	HTS-PDMS/Skin	6.5	0.05	0.75	4.0×4.0 cm^{-2}	[11]
Cellulose/PVA	VHB/Nylon	41	0.5	15	1.0×1.5 cm^{-2}	[12]
MGCSP organohydrogel	**PDMS/Skin**	**145**	**8.7**	**42.9**	**4.0×4.0 cm^{-2}**	**This work**

References

1. G. Tao, Y. Wang, R. Cai, H. Chang, K. Song, H. Zuo, P. Zhao, Q. Xia and H. He, *Mater Sci Eng C Mater Biol Appl*, 2019, **101**, 341-351.
2. H. Wei, Z. Wang, H. Zhang, Y. Huang, Z. Wang, Y. Zhou, B. B. Xu, S. Halila and J. Chen, *Chemistry of Materials*, 2021, **33**, 6731-6742.
3. Y. J. Liu, W. T. Cao, M. G. Ma and P. Wan, *ACS Appl Mater Interfaces*, 2017, **9**, 25559-25570.
4. K. Tian, J. Bae, S. E. Bakarich, C. Yang, R. D. Gately, G. M. Spinks, M. In Het Panhuis, Z. Suo and J. J. Vlassak, *Adv Mater*, 2017, **29,** 1604827.
5. C. Shao, M. Wang, L. Meng, H. Chang, B. Wang, F. Xu, J. Yang and P. Wan, *Chemistry of Materials*, 2018, **30**, 3110-3121.
6. G. Ge, W. Yuan, W. Zhao, Y. Lu, Y. Zhang, W. Wang, P. Chen, W. Huang, W. Si and X. Dong, *Journal of Materials Chemistry A*, 2019, **7**, 5949-5956.
7. Y. Zhou, C. Wan, Y. Yang, H. Yang, S. Wang, Z. Dai, K. Ji, H. Jiang, X. Chen and Y. Long, *Advanced Functional Materials*, 2019, **29**, 1806220.
8. L. Wang and W. A. Daoud, *Advanced Energy Materials*, 2018, 1803183.
9. Q. Guan, G. Lin, Y. Gong, J. Wang, W. Tan, D. Bao, Y. Liu, Z. You, X. Sun, Z. Wen and Y. Pan, *Journal of Materials Chemistry A*, 2019, **7**, 13948-13955.
10. T. Liu, M. Liu, S. Dou, J. Sun, Z. Cong, C. Jiang, C. Du, X. Pu, W. Hu and Z. L. Wang, *ACS nano*, 2018, **12**, 2818-2826.
11. Y. C. Lai, H. M. Wu, H. C. Lin, C. L. Chang, H. H. Chou, Y. C. Hsiao and Y. C. Wu, *Advanced Functional Materials*, 2019, **29,** 1904626.
12. Y. Wang, L. Zhang and A. Lu, *Journal of Materials Chemistry A*, 2020, **8**, 13935-13941.